Joint Calibrationless Reconstruction of Highly Undersampled Multi-Contrast MR Datasets Using Low-Rank Hankel Tensor Completion Framework

Zheyuan Yi[1,2,3†], Yilong Liu[1,2†], Yujiao Zhao[1,2], Linfang Xiao[1,2], Alex T. L. Leong[1,2], Yanqiu Feng[4], Fei Chen[3], and Ed X. Wu[1,2*]

[1]Laboratory of Biomedical Imaging and Signal Processing, the University of Hong Kong, Hong Kong SAR, People's Republic of China,

[2]Department of Electrical and Electronic Engineering, the University of Hong Kong, Hong Kong SAR, People's Republic of China,

[3]Department of Electrical and Electronic Engineering, Southern University of Science and Technology, Shenzhen, People's Republic of China

[4]School of Biomedical Engineering, Southern Medical University, Guangzhou, Guangdong, People's Republic of China

[*]Correspondence to:

Ed X. Wu, Ph.D.
Department of Electrical and Electronic Engineering
The University of Hong Kong, Hong Kong SAR, China
Tel: (852) 2859-7096
Fax: (852) 2559-8738
Email: ewu@eee.hku.hk

[†]These authors contributed equally to this work

Keywords: Multi-contrast, joint calibrationless reconstruction, low-rank, Hankel tensor completion

Yi Z, Liu Y, Zhao Y, Xiao L, Leong ATL, Feng Y, Chen F, Wu EX. Joint calibrationless reconstruction of highly undersampled multicontrast MR datasets using a low-rank Hankel tensor completion framework. Magn Reson Med. 2021 Jun;85(6):3256-3271. doi: 10.1002/mrm.28674.

Abstract

Purpose: To jointly reconstruct highly undersampled multi-contrast 2D datasets through a low-rank Hankel tensor completion (MC-HTC) framework.

Methods: MC-HTC is proposed to exploit the sharable information in multi-contrast datasets with respect to their highly correlated image structure, common spatial support, and shared coil sensitivity for joint reconstruction. This is achieved by firstly organizing multi-contrast k-space datasets into a single block-wise Hankel tensor. Subsequent low-rank tensor approximation via higher-order singular value decomposition (HOSVD) utilizes the image structural correlation by considering different contrasts as virtual channels. Meanwhile, the HOSVD imposes common spatial support and shared coil sensitivity by treating data from different contrasts as from additional k-space kernels. The missing k-space data are then recovered by iteratively performing such low-rank approximation and enforcing data consistency. This joint reconstruction framework was evaluated using multi-contrast multi-channel 2D human brain datasets (T1W, T2W, FLAIR, and T1W-IR) of identical image geometry with random and uniform undersampling schemes.

Results: The proposed method offered high acceleration, exhibiting significantly less residual errors when compared with both single-contrast SAKE and multi-contrast J-LORAKS low-rank reconstruction. Furthermore, MC-HTC was applied uniquely to Cartesian uniform undersampling by incorporating a novel complementary k-space sampling strategy where the phase-encoding direction among different contrasts is orthogonally alternated.

Conclusion: The proposed MC-HTC approach presents an effective tensor completion framework to jointly reconstruct highly undersampled multi-contrast 2D datasets without coil sensitivity calibration.

Introduction

Multi-contrast MRI has been routinely used in clinical settings for its capability of providing differential diagnostic information. At present, clinical MR session often acquires independent datasets of distinct contrast at the same slice location with various pulse sequences and parameter settings. However, such multiple and independent scans are time-consuming and increase the susceptibility to motion, especially with high spatial resolution and whole-brain coverage. Therefore, accelerating the multi-contrast data acquisition is highly desired.

Parallel imaging, which utilizes multiple receiver elements, has been commonly implemented to accelerate data acquisition beyond the Nyquist sampling rate. Conventional parallel imaging techniques[1-3] apply the encoding capability of receiving coils to reconstruct partially acquired data, thus requiring the coil sensitivity information for reconstruction. However, obtaining the coil sensitivity information either from calibration scan[1] or autocalibrating signals (ACS)[2] prolongs the acquisition time while the accuracy of such calibration data can be contaminated by motion, causing artifacts in reconstructed images[4]. Low-rank reconstruction has been recently proposed as the calibration-free alternative that avoids separate coil calibration procedures. These methods (such as SAKE, P-LORAKS, and ALOHA)[5-7] form the entire k-space data into a structured low-rank matrix to recover missing samples, which can inherently explore the underlying data relations from multi-channel acquisition and limited spatial support[8,9]. Although conventional parallel imaging and low-rank reconstruction enable fast imaging, the utilization of coil sensitivity and/or limited spatial support in single-contrast dataset alone may not be sufficient to achieve very high acceleration due to severe image artifacts and noise amplification.

Multi-contrast MR datasets share identical coil sensitivity[10] and possess highly correlated image structure[11] if acquired with identical geometry. Utilizing such sharable information in image reconstruction has been attempted to reduce residual artifacts and noise amplification. For example, shared coil sensitivity among multi-contrast images has been jointly estimated in parallel imaging by histogram entropy method[10] or through nonlinear inversion reconstruction[12]. However, these methods do not consider redundant structural information that is uniquely embedded in multi-contrast datasets.

To further exploit this information redundancy, parallel imaging has been combined with compressed sensing reconstruction[13,14] for additional regularizations on similar or consistent structural edges across different contrasts[15-23]. Additionally, the highly correlated anatomical structure among multi-contrast images ensures strong image content similarity. This image structural correlation has been explored as locally low-rank constraint[24], demonstrating applications in parameter mapping[25], dynamic imaging[26], and multi-contrast images denoising[27]. Recently, the higher-order tensor modeling has been adopted into image reconstruction for its advanced property such as the higher data compression ratio over matrix modeling[28,29]. For instance, an image-space locally low-rank approach[30], which forms a denoising tensor through block-matching of multi-contrast images, has been proposed. However, these image-space locally low-rank methods still require auto-calibration data, which can be vulnerable to inter-contrast inconsistency (e.g., caused by inter-scan motion).

Alternatively, calibrationless reconstruction has been expanded to utilize the sharable information in k-space that provides the first general application for multiple contrasts acquisitions[31]. This approach has considered k-space datasets from different contrasts as virtual channels[32,33] and then jointly reconstructed by GRAPPA (JVC-GRAPPA)[2,31] or low-rank matrix completion method (J-LORAKS)[8,31]. Additionally, a novel low-rank reconstruction method (HTC)[34] using the tensor expression for multi-channel k-space data has been shown to outperform conventional low-rank matrix completion, demonstrating the feasibility and potential of applying tensor modeling in k-space for reconstruction.

In this study, we propose to jointly reconstruct highly undersampled multi-contrast 2D k-space datasets through a novel block-wise Hankel tensor completion framework (MC-HTC). By combining the virtual channel concept for joint reconstruction[31], the proposed framework further provides a higher-order tensorial representation for multi-contrast datasets with the capability to take advantage of their highly correlated image structure, common spatial support, and shared coil sensitivity, which can lead to less residual errors especially at high acceleration. Moreover, MC-HTC can further incorporate a novel complementary sampling strategy where the phase-encoding direction among different contrasts is orthogonally alternated. While existing joint reconstruction methods[23,31,35] have demonstrated increased sampling incoherency by

using complementary undersampling patterns in multi-contrast data acquisition, MC-HTC with the proposed complementary sampling strategy can be applied even to uniform undersampling.

Theory

In the proposed MC-HTC framework, multi-contrast joint reconstruction is formulated as a low-rank tensor completion problem. This is achieved by structuring multi-contrast k-space data to a 3rd-order block-wise Hankel tensor (termed as a multi-contrast tensor in this study). Subsequent tensor decomposition and low-rank approximation serve to exploit sharable information for reconstruction, including highly correlated image structure, common spatial support, and shared coil sensitivity that resides naturally in multi-contrast datasets acquired with identical geometry.

Multilinear Low-rankness of Structured Multi-Contrast Tensor

In traditional auto-calibrating parallel imaging reconstruction[2,3,36], multi-channel k-space data exhibit strong linear relations that can be derived from calibration data and used for estimating missing k-space samples. Such linear relations generally arise from coil sensitivity modulation and limited spatial support of multi-channel MR images[37,38], which can be implicitly exploited in low-rank calibrationless reconstruction. Typically, the undersampled multi-channel k-space data has been organized as from different channels or kernels in a block-wise Hankel matrix to formulate calibrationless parallel imaging reconstruction as low-rank matrix completion. For further exploiting data relations across different contrasts, the block-wise Hankel matrices derived from individual contrasts can be concatenated into a larger matrix and then forced to be low-rank in J-LORAKS reconstruction[31]. Motivated by this virtual channel strategy and our recent HTC method[34], multi-contrast multi-channel k-space datasets can be formed into a 3rd-order tensor with multi-channel vectorized blocks across the entire k-space or from different contrasts aligned in kernel or contrast dimensions, respectively, as shown in Figure 1. Compared to the block-wise Hankel matrix from single-contrast MR data, the constructed tensor would potentially exhibit stronger multilinear low-rankness due to sharable information in multi-contrast datasets of identical geometry. The underlying

principle is to search a low-rank tensorial expression of multi-contrast k-space datasets (denoted as X) to estimate the missing k-space samples. Therefore, joint reconstruction can be formulated as a constrained minimization problem. Here, Y is the acquired multi-contrast data and D corresponds to the sampling pattern. P denotes the operator that constructs multi-contrast tensor (denoted as Γ) from multi-channel multi-contrast k-space data. $||\cdot||_F^2$ denotes the Frobenius norm to guarantee data fidelity.

$$\begin{aligned} &minimize\ rank(\Gamma) \\ &s.t.\quad \Gamma = PX,\ \ \|DX - Y\|_F^2 < \varepsilon \end{aligned} \qquad [1]$$

To capture the underlying data relations with low-rank approximation, this study performs the higher-order singular value decomposition (HOSVD)[39] (also known as Tucker decomposition[40,41]) to analyze the multilinear subspace of multi-contrast tensor. This type of decomposition derives a core tensor S together with n-mode (n = 1, 2, and 3) unitary matrices $U^{(n)}$. Hence, the reconstruction problem in Equation [1] can be reformulated as following with the targeted rank of multi-contrast tensor empirically selected beforehand. Here, P^{-1} represents the pseudo-inverse operator that converts the tensor back to k-space datasets with each sample obtained by averaging its corresponding elements in multi-contrast tensor. The multilinear rank restricts unitary matrices $U^{(1)}$, $U^{(2)}$, and $U^{(3)}$ to their first r_1, r_2, and r_3 column vectors that span the signal subspaces corresponding to n-mode (n = 1, 2, and 3) matrix unfolding[39] of multi-contrast tensor, respectively.

$$\begin{aligned} &\underset{\Gamma}{argmin}\ \|DP^{-1}\Gamma - Y\|_F^2 \\ &s.t.\quad \Gamma = S \times_1 U^{(1)} \times_2 U^{(2)} \times_3 U^{(3)} \end{aligned} \qquad [2]$$

Note that two important characteristics are embedded in this joint reconstruction. First, low-rank features within individual contrast data are incorporated by forming the channel and kernel dimensions of multi-contrast tensor based on conventional low-rank methods[5,6]. Second, common low-rank features (sharable information) corresponding to each dimension of the multi-contrast tensor are decomposed separately into different modes of unitary matrices. These two characteristics would provide more accurate and complementary data relations for reconstructing highly undersampled multi-contrast

datasets.

Exploiting Highly Correlated Image Structure

As shown in Figure 2, the HOSVD in this study is conducted by sequentially applying the singular value decomposition to n-mode matrix unfolding (denoted as $\Gamma_{(n)}$) of the multi-contrast tensor[42]. Specifically, the 1-mode unitary matrix is derived by a two-step procedure. The contrast dimension with arbitrary N_{con} contrasts is stacked along the channel dimension with arbitrary N_{ch} channels to form the 1-mode matrix unfolding $\Gamma_{(1)}$ with total $N_{con} \times N_{ch}$ channels, followed by SVD to compute $U^{(1)}$.

$$\Gamma_{(n)} = U^{(n)} \Sigma^{(n)} V^{(n)^H} \quad [3]$$

Underlying this unfolding is to jointly reconstruct the datasets by regarding different contrast as virtual channels. Note that these virtual channels exhibit strong image structural correlation due to the same slice geometry and field-of-view in multi-contrast data acquisition. From this perspective, enforcing the low-rankness of $\Gamma_{(1)}$ inherently exploits image structural correlation, which can also be interpreted as fulfilling the smoothness of coil sensitivity across virtual channels in low-rank reconstruction[5,6,38]. Similar strategy has been implemented in the J-LORAKS[31] method for reconstructing multi-contrast datasets. In theory, reconstruction with virtual channel strategy alone is equivalent to a degenerated Tucker1 model[43] of HOSVD in this tensor modeling by assuming both $U^{(2)}$ and $U^{(3)}$ in Equation [2] to be the identity matrix. Importantly, the 2-mode matrix unfolding of the tensor should also be inherently rank-deficient (Supporting Information Figure S1) due to common spatial support and shared coil sensitivity among contrasts and incorporated in this study for more accurate low-rank approximation.

Exploiting Common Spatial Support and Shared Coil Sensitivity

As illustrated in Figure 2, the 2-mode unitary matrix $U^{(2)}$ is obtained similarly by unfolding the contrast dimension with N_{con} contrasts into the kernel dimension with N_k kernels, resulting in total $N_{con} \times N_k$ kernels in the 2-mode matrix unfolding $\Gamma_{(2)}$. This unfolding operation can be interpreted as generating “virtual kernels” by further using

the k-space data from different contrasts when compared to the single-contrast low-rank matrix completion method (P-LORAKS and SAKE)[5,6]. While the null subspace of the block-wise Hankel matrix can capture the constraint of limited spatial support, promoting low-rankness to $\Gamma_{(2)}$ with virtual kernels would generalize common spatial support constraint for all contrasts. Furthermore, different contrast data acquired from the same receiver coils are also aligned across the channel dimension as indicated in Figure 2. For this consideration, virtual kernels would also share coil sensitivity information by simultaneously identifying a common signal subspace of $\Gamma_{(2)}$ and forcing all vectorized kernels to lie in that low-dimensional subspace. This is conceptually similar to the ESPIRiT method[44] that derives the signal subspace from data blocks within the auto-calibration region to estimate coil sensitivity maps. Additionally, the undersampling patterns are required to be sufficiently incoherent to identify data relations that existed among different k-space kernels for low-rank reconstruction. Note that virtual kernels derived from different contrasts are capable to possess complementary undersampling patterns that can significantly increase incoherency, especially for uniform undersampling.

In this study, $\Gamma_{(3)}$ formed by unfolding channel and kernel dimensions of the tensor is determined to be full-rank without any nullspace vector (Supporting Information Figure S1). This implies the distinct contrast information and the low-rank tensor approximation problem in Equation [2] can be further simplified by ignoring the 3-mode unfolding.

$$\begin{aligned} &\underset{\Gamma}{argmin} \; \|DP^{-1}\Gamma - Y\|_F^2 \\ &s.t. \quad rank(\Gamma) = (r_1,\, r_2,\, N_{con}) \end{aligned} \qquad [4]$$

where N_{con} represents the number of contrasts (4 in this study) to be jointly reconstructed. The simplified Tucker2 model[43] can also be solved efficiently via alternating direction method of multipliers (ADMM)[45]. Although $\Gamma_{(3)}$ in this study is not exploited for simplicity, data relations corresponding to the contrast dimension of the tensor would potentially lead to the low-rankness in other applications like T_2 and T_2^* parameter mapping[31,46].

Methods

Multi-Contrast Hankel Tensor Completion Framework

For implementing previously described joint multi-contrast MR reconstruction, the MC-HTC framework proceeds iteratively until convergence as follows (Figure 1):

Multi-contrast tensor construction: Similar to conventional low-rank matrix completion methods[5-7], multi-channel vectorized blocks are selected by sliding a window across the entire k-space and from different contrasts[31], then spanned along additional kernel and contrast dimensions, respectively, forming a 3rd-order multi-contrast tensor Γ.

Multilinear low-rank tensor approximation: The multi-contrast tensor manifests strong low-rankness and thus can be compressed by sequentially applying different modes of tensor unfolding together with truncated matrix SVD[42] that restricting the decomposed unitary matrices to be their first r_1, r_2, and r_3 column vectors. After that, the multilinear multiplication[39] of $U^{(1)}$, $U^{(2)}$, $U^{(3)}$ and S is performed to regenerate the low-rank approximated multi-contrast tensor.

Consistencies projection: To find out the solution of the defined constrained optimization problem, the projection-onto-sets algorithm has been implemented that directly projects the low-rank approximated data to the least-square solution for each iteration. This procedure requires the conversion of the tensor back to sets of k-space kernels which simultaneously imposes the consistency of block-wise Hankel structure and enforces strict data consistency.

Data Acquisition and Retrospective Undersampling

Reconstruction performance was evaluated by using the raw 2D Cartesian brain datasets, collected on a 3T scanner (Philips Healthcare, Best, Netherland) using an 8-channel head coil. Fully sampled datasets of four typical MRI contrasts were acquired with identical locations. For T1-weighted (T1W) acquisition, 2D fast field echo (FFE) was used with TE/TR = 4/519 ms, and flip angle = 80°. For T2-weighted (T2W), fluid-attenuated inversion recovery (FLAIR), and T1-weighted inversion recovery (T1W-IR)

acquisitions, 2D fast spin echo (FSE) was used with TE/TR = 86/3000 ms, TE/TI/TR = 135/2500/8000 ms, and TE/TI/TR = 20/800/2000 ms, respectively. Other imaging parameters were acquisition matrix size = 300 × 300, image matrix 200 × 200 by cropping, image FOV = 240 × 240 mm^2, and slice gap/thickness = 1/4 mm for all datasets.

Multi-contrast k-space data were retrospectively undersampled with several undersampling schemes. By discarding some phase-encoding lines according to the acceleration factor (R = 4), 1D random undersampling patterns were independently generated for each contrast. The proposed MC-HTC was performed on single (T1W or T2W), two (T1W and T2W), three (T1W, T2W, and FLAIR), and four (T1W, T2W, FLAIR, and T1W-IR) contrasts to examine reconstruction with the increased contrast number. Typical calibrationless 2D Poisson-disc undersampling patterns (R = 8) were also independently generated for each contrast to evaluate reconstruction. To further demonstrate the potential of MC-HTC, the Cartesian uniform 1D undersampling patterns (R = 4) were applied with alternated phase-encoding directions among different contrasts. The MC-HTC was performed on five different slices using the aforementioned 1D and 2D undersampling schemes with acceleration factors from 3 to 5 and 6 to 9, respectively.

Reconstruction for multi-contrast datasets with simulated rigid inter-scan motion was also conducted. For T2W, FLAIR, and T1W-IR datasets, images were manually displaced along the frequency-encoding, phase-encoding, and both directions, respectively, with displacement set to 2 or 4 pixels (corresponding to 2.4mm or 4.8mm).

The results were compared to both single-contrast SAKE[5] and multi-contrast J-LORAKS[31] reconstruction. For J-LORAKS, the 'S'-version of non-convex P-LORAKS method[6] was performed preliminarily for each contrast data to generate an initial reconstruction as suggested[47]. The rank values for MC-HTC, J-LORAKS, and SAKE were empirically optimized to guarantee the optimal performance (Supporting Information Table S1). The reconstruction was terminated with the same criterion of updating tolerance that ensures the convergence in all methods. To assess image quality, residual error maps were derived by subtracting reconstructed images channel-by-channel from fully sampled references and then sum-of-square combined. To examine the error distributions, the histograms were also calculated for the 1D random

undersampling scheme. The quantitative assessment was also performed for all undersampling schemes by measuring the normalized root-mean-square errors (NRMSE)[20] within the object region.

Results

Figure 3 illustrates the performance of MC-HTC and J-LORAKS reconstruction with increased number of contrasts using 1D random undersampling patterns. Note that MC-HTC and J-LORAKS applications for individual T1W data became conventional single-contrast reconstruction, leading to severe aliasing and noise-like residual errors. MC-HTC joint reconstruction with two contrasts substantially reduced aliasing, producing relatively clear image details with less residual errors compared to that in J-LORAKS results. With three or four contrasts reconstructed jointly, image structural details were almost fully recovered in MC-HTC and no apparent leakage was observed among contrasts.

Comparisons to J-LORAKS reconstruction with 1D random undersampling patterns are shown in Figure 4. MC-HTC produced high-quality images with clear details for all contrasts and yielded nearly 30% improvement in terms of NRMSE. As illustrated in brightened error maps, the noise-like residuals were effectively suppressed in MC-HTC results, especially for the FLAIR image which has relatively low SNR.

Figure 5 further depicts the reconstruction errors for MC-HTC, J-LORAKS, and single-contrast SAKE reconstruction with 1D random undersampling patterns. The large residual errors related to aliasing artifacts were significantly reduced through MC-HTC. Apart from aliasing, SAKE and J-LORAKS also showed noticeable noise-like residuals (indicated by the majority of errors) associated with the vulnerability of noise at high acceleration, which is effectively mitigated by MC-HTC reconstruction.

Figure 6 shows the typical performance of MC-MTC joint reconstruction with 2D Poisson-disc undersampling patterns at high acceleration (R = 8). MC-HTC provided better image quality for all contrasts with noise-like artifacts effectively suppressed when compared to J-LORAKS results.

Figure 7 demonstrates the applicability of MC-HTC joint reconstruction to the completely uniform undersampling patterns while alternating the phase-encoding direction among contrasts. Low-rank J-LORAKS reconstruction could not handle such highly coherent undersampling patterns here, yet MC-HTC yielded high-quality images with levels of aliasing and noise-like errors comparable to those in Figure 4.

Figure 8 summarizes the overall performances in terms of averaged NRMSEs in five different slices. MC-HTC joint reconstruction consistently outperformed SAKE and J-LORAKS methods with all aforementioned undersampling patterns, especially at high acceleration factors.

Figure 9 demonstrates the tolerance of MC-HTC to rigid inter-scan motion. As shown in error maps, J-LORAKS reconstruction is more sensitive to such simulated in-plane motion with NRMSE increased by nearly 0.02 from 2-pixel to 4-pixel displacement. Meanwhile, MC-HTC reconstruction increased NRMSE by only 0.007, which was negligible. With 4-pixel corresponding to 4.8mm displacement, both SAKE and J-LORAKS reconstruction suffered from severe residual errors, whereas MC-HTC still produced promising T1W images with preserved structural details and edges.

Discussion

This study presents a calibrationless joint reconstruction framework to exploit the sharable information in highly undersampled multi-contrast datasets. The proposed MC-HTC framework constructs the datasets into a higher-order block-wise Hankel tensor and enforces its multilinear low-rankness via HOSVD. Specifically, the tensor decomposition treats different contrasts as from virtual k-space channels[31] to provide the low-rank constraint on highly correlated image structure while imposing common spatial support and shared coil sensitivity by treating different contrast data as from virtual k-space kernels. This approach can achieve higher acceleration and outperforms both the single-contrast SAKE and multi-contrast J-LORAKS methods. Moreover, this joint reconstruction approach is capable to take advantage of the sampling incoherency created by orthogonally alternating the phase-encoding direction among contrasts.

Utilizing Multi-Contrast Sharable Information for High Acceleration

In conventional parallel imaging and low-rank techniques, the noise amplification undermines the accuracy of data estimation that inherently limits the achievable acceleration factor. In this study, joint reconstruction demonstrates the effectiveness of reducing noise-like residuals for all contrasts and enables the acceleration beyond what single-contrast SAKE or multi-contrast J-LORAKS reconstruction can offer (see Figure 5 and Supporting Information Figure S2). Such improvement over SAKE arises in part from the exploitation of image structural correlation among virtual channels, which have been demonstrated by the J-LORAKS method. Random noise is uncorrelated across different contrasts and will be suppressed by enforcing the low-rankness. Although the SNR improvement through virtual contrast channels was not directly comparable to that achieved by real channels, the reduction of noise-like residual was still significant with the increasing number of contrasts jointly reconstructed (Figure 3 and Supporting Information Figure S3).

Moreover, the data-driven low-rank approximation can become inaccurate at high acceleration and incur obvious aliasing. Our proposed joint reconstruction exploits linear relations shared among different virtual k-space kernels that can be interpreted as providing common spatial support constraint for all contrasts, leading to substantially reduced aliasing artifacts (Figure 5 and Supporting Information Figure S2). The feature of common convolutional relations has also been utilized in conventional parallel imaging that adjacent slices[48] can share the same sets of convolutional kernels. In MC-HTC joint reconstruction, the improved k-space estimation also partially arises from sharing coil sensitivity information among aligned channels (Figure 2). To demonstrate the effectiveness of sharing coil sensitivity information, we deliberately introduced severe inconsistency of coil sensitivity among T1W and other contrasts by swapping 2 channels of T1W data before forming the structured low-rank tensor (Supporting Information Figure S4). In MC-HTC, this swapping caused misalignment of channels, leading to artifacts to the reconstructed T1W image within the region where existed severe coil sensitivity mismatch. Note that the image quality of MC-HTC results for the other contrasts (T2W, FLAIR, and T1W-IR) was still promising with only slightly increased artifacts, suggesting that the proposed reconstruction method may tolerate the minor mismatch of coil sensitivity among contrasts in practice.

Comparing with Existing Multi-Contrast Reconstruction Approaches

Several recent multi-contrast reconstruction approaches[22,23,49] have utilized image structural correlation based on compressed sensing and made improvements over single-contrast reconstruction. In contrast, the proposed MC-HTC exploits the low-rank characteristic of multi-contrast tensor for reconstruction without requiring calibration or additional prior information. Moreover, the low-rankness enforced in MC-HTC only identifies common linear relations of k-space samples to recover missing data, thus it is expected to be more resilient to slight inter-scan motion compared to those with strong modeling assumptions on sparsity patterns or locations of image structure[22,23]. In general, low-rank and compressed sensing reconstruction are two categories of methods, and MC-HTC can be extended to incorporate spatial regularity[50] for further improvements.

In MC-HTC, the virtual channel concept utilized by the 1-mode unfolding is essentially the same as adopted from J-LORAKS reconstruction. However, J-LORAKS requires proper initialization by reconstructing the central k-space subregion or individual reconstruction of each contrast for acceleration[31,47]. Such initializations were motivated by the fact that the matrix concatenated with virtual channels has a much larger signal subspace, making joint reconstruction hard to converge. Due to identical coil sensitivity and spatial support, the 2-mode matrix unfolding has the rank close to that for the single-contrast reconstruction (Supporting Information Figure S1). Sequentially enforcing low-rankness for 1-/2- mode matrix unfolding can accelerate the convergence and avoid manual initialization. Note that J-LORAKS is also more sensitive to noise as suggested by the reconstructed FLAIR images with relatively low-SNR (Figure 4 and 6).

More importantly, virtual kernels derived from different contrasts can have orthogonal k-space undersampling patterns, which makes MC-HTC applicable to uniformly undersampled data (Figure 7). As revealed in some early studies[51,52], the structured low-rank matrix completion problem is ill-conditioned with extremely coherent uniform undersampling patterns and may reach the local minimum without a good initialization or additional prior information. However, by incorporating complementary undersampling patterns, the coherency of artifacts can be mitigated as revealed by some compressed sensing reconstruction approaches[13,14,23]. In this study, we have further

enhanced the complementary sampling strategy by orthogonally alternating the phase-encoding directions among contrasts, forming 'pseudo-2D' sampling patterns in multi-contrast data acquisition. The effects of pseudo-2D undersampling were demonstrated by the obvious leakage of artifacts from other contrasts for the first few iterations in MC-HTC reconstruction (Supporting Information Figure S5) and the estimated 2D common spatial support (Supporting Information Figure S6). As a result, MC-HTC reconstruction with this novel complementary uniform sampling can converge stably with different types of initializations, such as zeros, additive white Gaussian noise, or ill-conditioned single-contrast reconstruction (Supporting Information Figure S7).

MC-HTC is expected to apply for scenarios where acquiring calibration data is inefficient or error-prone as in abdominal imaging, or uniform undersampling is desired or a must as in popular SENSE and echo planar imaging (EPI) acquisitions[29,53]. For anisotropic FOV, the spacings of acquired k-space samples need to be alternated simultaneously with the readout and phase-encoding directions to maintain the desired spatial resolution that may lead to increased phase-encoding steps. Note that severe inter-contrast inconsistency can be induced by alternating the phase-encoding direction (e.g., mismatch of geometric distortion in echo-planar imaging), which may significantly undermine the joint reconstruction. However, as revealed in some early studies, the mismatch of geometric distortion and inter-scan motion caused by alternating the phase-encoding direction can be corrected or substantially mitigated[54,55]. Additionally, our proposed MC-HTC can still outperform SAKE and J-LORAKS reconstruction in the presence of minor inter-scan motion (Figure 9), suggesting its robustness in practice.

Generalization and Extension of MC-HTC Framework

Note that the proposed MC-HTC in this study is not a direct 4th-order extension of HTC[34]. This earlier approach treats different channels as an independent dimension, which can further enhance the improvements but inevitably increase complexity and computational burden in a prohibitive manner. In the present MC-HTC approach, formulating multi-contrast reconstruction as an efficient 3rd-order low-rank tensor completion problem can synergistically explore highly correlated image structure, common spatial support, and shared coil sensitivity that provides a good tradeoff

between complexity and performance. Owing to the exploitation of such multi-contrast sharable information, the proposed MC-HTC framework can also be generalized to other applications, such as perfusion imaging or multi-echo imaging. Similar to MC-HTC, a higher-order Hankel tensor with frame or echo dimension can be constructed accordingly. Note that 3-mode matrix unfolding of the tensor may also be low-rank in these potential applications and can be incorporated to further improve the reconstruction. Moreover, the formulation of joint reconstruction can easily accommodate additional regularizations such as the phase constraint[56]. One example is that multi-contrast tensor can be constructed by concatenating the "S matrix" in J-LORAKS method[6,31] that provides the smoothly varied phase constraint of each contrast data and extends the application for partial Fourier acquisition.

Reconstruction Parameters and Computational Times

The performance of the proposed method depends on several reconstruction parameters, including the kernel size, iteration number, and target rank. Similar to single-contrast low-rank approaches[5,8], increasing the kernel size can lead to a slight improvement of reconstruction at the expense of computation. Using a personal desktop (4-core i5-6500 and 16GB RAM), the proposed method required about 30, 20, and 40 minutes per slice to converge for all four contrasts (8-channel datasets) with 1D random, 2D random, and 1D uniform undersampling patterns, respectively. The computational speed can also be accelerated by incorporating recent advances for efficient low-rank approximation[57,58]. The iteration number and target rank were empirically determined to guarantee optimal performance in this study. Generally, the 2-mode rank of the multi-contrast tensor depends on spatial support, coil sensitivity, and the size of the sliding window for tensor construction. Its selection should be similar to that in conventional single-contrast approaches[5,6]. Note that the multilinear rank (1- and 3-mode unfolding) would also rely on the number of jointly reconstructed contrasts and the similarity/correlation of image contents among contrasts. Automatic parameter selection is valuable for practical implementation and deserves investigation in future studies.

Conclusion

This study presents a novel calibrationless joint reconstruction framework, MC-HTC, for highly undersampled multi-contrast 2D datasets. This low-rank tensor completion approach exploits highly correlated anatomical structure, common spatial support, and shared coil sensitivity, leading to significantly less residual errors at high acceleration. In practice, the MC-HTC approach can be readily combined with the undersampling pattern variations among contrasts to further reduce residual errors or increase acceleration.

Acknowledgments

This study is supported in part by Hong Kong Research Grant Council (R7003-19/C7048-16G/HKU17112120 to E.X.W. and HKU17103819/HKU17104020 to A.T.L.), Guangdong Key Technologies for Treatment of Brain Disorders (2018B030332001 to E.X.W.), Guangdong Key Technologies for Alzheimer's Disease Diagnosis and Treatment (2018B030336001 to E.X.W.), and Guangdong-Hong Kong-Macao Greater Bay Area Center for Brain Science and Brain-Inspired Intelligence Fund (2019008).

Reference

[1] Pruessmann KP, Weiger M, Scheidegger MB, Boesiger P. SENSE: Sensitivity encoding for fast MRI. Magn Reson Med 1999;42(5):952-962.

[2] Griswold MA, Jakob PM, Heidemann RM, Nittka M, Jellus V, Wang J, Kiefer B, Haase A. Generalized autocalibrating partially parallel acquisitions (GRAPPA). Magn Reson Med 2002;47(6):1202-1210.

[3] Lustig M, Pauly JM. SPIRiT: Iterative self-consistent parallel imaging reconstruction from arbitrary k-space. Magn Reson Med 2010;64(2):457-471.

[4] Blaimer M, Breuer F, Mueller M, Heidemann RM, Griswold MA, Jakob PM. SMASH, SENSE, PILS, GRAPPA: how to choose the optimal method. Top Magn Reson Imaging 2004;15(4):223-236.

[5] Shin PJ, Larson PEZ, Ohliger MA, Elad M, Pauly JM, Vigneron DB, Lustig M. Calibrationless parallel imaging reconstruction based on structured low-

rank matrix completion. Magn Reson Med 2014;72(4):959-970.

[6] Haldar JP, Zhuo J. P-LORAKS: Low-rank modeling of local k-space neighborhoods with parallel imaging data. Magn Reson Med 2016;75(4):1499-1514.

[7] Lee D, Jin KH, Kim EY, Park SH, Ye JC. Acceleration of MR parameter mapping using annihilating filter-based low rank hankel matrix (ALOHA). Magn Reson Med 2016;76(6):1848-1864.

[8] Haldar JP. Low-Rank Modeling of Local k-Space Neighborhoods (LORAKS) for Constrained MRI. IEEE Trans Med Imaging 2014;33(3):668-681.

[9] Plevritis SK, Macovski A. Spectral extrapolation of spatially bounded images [MRI application]. IEEE Trans Med Imaging 1995;14(3):487-497.

[10] Li Y, Dumoulin C. Correlation imaging for multiscan MRI with parallel data acquisition. Magn Reson Med 2012;68(6):2005-2017.

[11] Huang J, Chen C, Axel L. Fast multi-contrast MRI reconstruction. Magn Reson Med 2014;32(10):1344-1352.

[12] Uecker M, Hohage T, Block KT, Frahm J. Image reconstruction by regularized nonlinear inversion-joint estimation of coil sensitivities and image content. Magn Reson Med 2008;60(3):674-682.

[13] Lustig M, Donoho D, Pauly JM. Multi-slice compressed sensing imaging. In: Proceedings of the 15th Annual Meeting of ISMRM, Berlin, Germany, 2007, p 828.

[14] Lustig M, Donoho D, Pauly JM. Sparse MRI: The application of compressed sensing for rapid MR imaging. Magn Reson Med 2007;58(6):1182-1195.

[15] Haldar JP, Liang Z. Joint reconstruction of noisy high-resolution MR image sequences. In: 5th IEEE International Symposium on Biomedical Imaging: From Nano to Macro, Paris, France, 2008, p 752-755.

[16] Otazo R, Kim D, Axel L, Sodickson DK. Combination of compressed sensing and parallel imaging for highly accelerated first-pass cardiac perfusion MRI. Magn Reson Med 2010;64(3):767-776.

[17] Trzasko JD, Manduca A. Group Sparse Reconstruction of Vector-Valued Images. In: Proceedings of the 19th Annual Meeting of ISMRM, Montreal, QC, Canada, 2011, p 2839.

[18] Bilgic B, Goyal VK, Adalsteinsson E. Multi-contrast reconstruction with Bayesian compressed sensing. Magn Reson Med 2011;66(6):1601-1615.

[19] Haldar JP, Wedeen VJ, Nezamzadeh M, Dai G, Weiner MW, Schuff N, Liang Z. Improved diffusion imaging through SNR-enhancing joint reconstruction. Magn Reson Med 2013;69(1):277-289.

[20] Gong E, Huang F, Ying K, Wu W, Wang S, Yuan C. PROMISE: Parallel-imaging and compressed-sensing reconstruction of multicontrast imaging using SharablE information. Magn Reson Med 2015;73(2):523-535.

[21] Shi X, Ma X, Wu W, Huang F, Yuan C, Guo H. Parallel imaging and compressed sensing combined framework for accelerating high-resolution diffusion tensor imaging using inter-image correlation. Magn Reson Med 2015;73(5):1775-1785.

[22] Datta S, Deka B. Multi-channel, multi-slice, and multi-contrast compressed sensing MRI using weighted forest sparsity and joint TV regularization priors. In: Soft Computing for Problem Solving, 2019, Springer, p 821-832.

[23] Kopanoglu E, Güngör A, Kilic T, Saritas EU, Oguz KK, Çukur T, Güven HE. Simultaneous use of individual and joint regularization terms in compressive sensing: Joint reconstruction of multi-channel multi-contrast MRI acquisitions. NMR Biomed 2020;33(4):e4247.

[24] Trzasko JD, Manduca A, Borisch EA. Local versus global low-rank promotion in dynamic MRI series reconstruction. In: Proceedings of the 19th Annual Meeting of ISMRM, Montréal, Québec, Canada, 2011, p 4371.

[25] Zhang T, Pauly JM, Levesque IR. Accelerating parameter mapping with a locally low rank constraint. Magn Reson Med 2015;73(2):655-661.

[26] Zhang T, Cheng JY, Potnick AG, Barth RA, Alley MT, Uecker M, Lustig M, Pauly JM, Vasanawala SS. Fast pediatric 3D free-breathing abdominal dynamic contrast enhanced MRI with high spatiotemporal resolution. J Magn Reson Imaging 2015;41(2):460-473.

[27] Zhao Y, Liu Y, Mak H, Wu E. Simultaneous Denoising of Multi-contrast MR Imaging Using a Novel Weighted Nuclear Norm Minimization Approach. In: Proceedings of the 27th Annual Meeting of ISMRM, Montreal, QC, Canada, 2019, p 669.

[28] Yu Y, Jin J, Liu F, Crozier S. Multidimensional compressed sensing MRI using tensor decomposition-based sparsifying transform. PloS One 2014;9(6):e98441.

[29] Banco D, Aeron S, Hoge WS. Sampling and recovery of MRI data using low rank tensor models. In: 38th Annual International Conference of the IEEE Engineering in Medicine and Biology Society (EMBC), Orlando, Florida USA, 2016, p 448-452.

[30] Bustin A, Jaubert O, Lopez K, Botnar R, Prieto C. High-dimensionality undersampled patch-based reconstruction (HD-PROST) for accelerated multi-contrast MRI. Magn Reson Med 2019;81(6):3705-3719.

[31] Bilgic B, Kim TH, Liao C, Manhard MK, Wald LL, Haldar JP, Setsompop K. Improving parallel imaging by jointly reconstructing multi-contrast data. Magn Reson Med 2018;80(2):619-632.

[32] Blaimer M, Gutberlet M, Kellman P, Breuer FA, Köstler H, Griswold MA. Virtual coil concept for improved parallel MRI employing conjugate symmetric signals. Magn Reson Med 2009;61(1):93-102.

[33] Liu Y, Lyu M, Barth M, Yi Z, Leong AT, Chen F, Feng Y, Wu EX. PEC-GRAPPA reconstruction of simultaneous multislice EPI with slice-dependent 2D Nyquist ghost correction. Magn Reson Med 2019;81(3):1924-1934.

[34] Liu Y, Cao J, Lyu M, Wu E. Calibration-less parallel imaging reconstruction using hankel tensor completion (HTC). In: Proceedings of the 25th Annual Meeting of ISMRM, Honolulu, HI, USA, 2017, p 445.

[35] Mani M, Jacob M, McKinnon G, Yang B, Rutt B, Kerr A, Magnotta V. SMS MUSSELS: A navigator-free reconstruction for simultaneous multi-slice-accelerated multi-shot diffusion weighted imaging. Magn Reson Med 2020;83(1):154-169.

[36] Heidemann RM, Griswold MA, Haase A, Jakob PM. VD-AUTO-SMASH imaging. Magn Reson Med 2001;45(6):1066-1074.

[37] Ye JC. Compressed sensing MRI: a review from signal processing perspective. BMC Biomedical Engineering 2019;1(1):8.

[38] Haldar JP, Setsompop K. Linear Predictability in Magnetic Resonance Imaging Reconstruction: Leveraging Shift-Invariant Fourier Structure for Faster and Better Imaging. IEEE Signal Processing Magazine 2020;37(1):69-82.

[39] De Lathauwer L, De Moor B, Vandewalle J. A multilinear singular value decomposition. SIAM Journal on Matrix Analysis and Applications 2000;21(4):1253-1278.

[40] Tucker LR. Some mathematical notes on three-mode factor analysis. Psychometrika 1966;31(3):279-311.

[41] Kolda TG, Bader BW. Tensor Decompositions and Applications. SIAM Review 2009;51(3):455-500.

[42] Vannieuwenhoven N, Vandebril R, Meerbergen K. A new truncation strategy for the higher-order singular value decomposition. SIAM Journal on Scientific Computing 2012;34(2):A1027-A1052.

[43] Acar E, Yener B. Unsupervised multiway data analysis: A literature survey. IEEE Transactions on Knowledge and Data Engineering 2008;21(1):6-20.

[44] Uecker M, Lai P, Murphy MJ, Virtue P, Elad M, Pauly JM, Vasanawala SS, Lustig M. ESPIRiT-an eigenvalue approach to autocalibrating parallel MRI: where SENSE meets GRAPPA. Magn Reson Med 2014;71(3):990-1001.

[45] Yi Z, Liu Y, Chen F, Wu E. Joint Calibrationless Reconstruction of Highly Undersampled Multi-contrast MR Datasets Using A Novel Low-Rank

Completion Approach. In: Proceedings of the 27th Annual Meeting of ISMRM, Montreal, QC, Canada, 2019, p 4746.

[46] Sumpf TJ, Uecker M, Boretius S, Frahm J. Model-based nonlinear inverse reconstruction for T2 mapping using highly undersampled spin-echo MRI. J Magn Reson Imaging 2011;34(2):420-428.

[47] Kim TH, Garg P, Haldar JP. LORAKI: Autocalibrated recurrent neural networks for autoregressive MRI reconstruction in k-space. arXiv preprint 2019;arXiv:1904.09390.

[48] Honal M, Bauer S, Ludwig U, Leupold J. Increasing efficiency of parallel imaging for 2D multislice acquisitions. Magn Reson Med 2009;61(6):1459-1470.

[49] Chatnuntawech I, Martin A, Bilgic B, Setsompop K, Adalsteinsson E, Schiavi E. Vectorial total generalized variation for accelerated multi-channel multi-contrast MRI. Magn Reson Imaging 2016;34(8):1161-1170.

[50] Holler M, Huber R, Knoll F. Coupled regularization with multiple data discrepancies. Inverse Probl 2018;34(8):084003.

[51] Kim TH, Setsompop K, Haldar JP. LORAKS makes better SENSE: phase-constrained partial fourier SENSE reconstruction without phase calibration. Magn Reson Med 2017;77(3):1021-1035.

[52] Lobos RA, Kim TH, Hoge WS, Haldar JP. Navigator-free EPI ghost correction with structured low-rank matrix models: New theory and methods. IEEE Trans Med Imaging 2018;37(11):2390-2402.

[53] Ravishankar S, Bresler Y. Adaptive sampling design for compressed sensing MRI. In: 33rd Conference Proceedings IEEE Engineering Medicine Biology Society (EMBC), Boston, Massachusetts, USA, 2011, p 3751-3755.

[54] Kruger DG, Slavin GS, Muthupillai R, Grimm RC, Riederer SJ. An orthogonal correlation algorithm for ghost reduction in MRI. Magn Reson Med 1997;38(4):678-686.

[55] Cordes D, Arfanakis K, Haughton V, Meyerand M. Geometric distortion correction in EPI using two images with orthogonal phase-encoding directions. In: Proceedings of the 8th Annual Meeting of ISMRM, Denver, 2000, p 1712.

[56] MacFall JR, Pelc NJ, Vavrek RM. Correction of spatially dependent phase shifts for partial Fourier imaging. Magn Reson Imaging 1988;6(2):143-155.

[57] Ongie G, Jacob M. A Fast Algorithm for Convolutional Structured Low-Rank Matrix Recovery. IEEE Transactions on Computational Imaging 2017;3(4):535-550.

[58] Kim TH, Bilgic B, Polak D, Setsompop K, Haldar JP. Wave-LORAKS:

Combining wave encoding with structured low-rank matrix modeling for more highly accelerated 3D imaging. Magn Reson Med 2019;81(3):1620-1633.

Figure Captions

Figure 1. Diagram of the proposed MC-HTC framework. The multi-contrast k-space data can be constructed into a block-wise Hankel tensor, with the multi-channel vectorized blocks across the entire k-space or from different contrasts aligned in kernel or contrast dimensions, respectively. The inherent low-rankness of such constructed tensor is then explored by multilinear low-rank approximation via HOSVD, which restricts the decomposed unitary matrices to be first r_1, r_2, and r_3 column vectors. The missing k-space samples are iteratively updated by enforcing the low-rankness, while repeatedly promoting the structural and data consistencies by regenerating k-space data from the multi-contrast tensor.

Figure 2. Illustration of HOSVD to multi-contrast tensor. The unitary matrices can be derived by a two-step procedure. Specifically, for the 1-mode matrix unfolding, different contrasts are regarded as from virtual channels and then matrix SVD exploits data relations among all channels. Similarly, virtual kernels from different contrasts are concatenated in the 2-mode matrix unfolding, enabling common data relations among all kernels to be exploited. The 3-mode unfolding is determined to be full-rank and thus not considered for simplicity.

Figure 3. Reconstruction with 1-, 2-, 3-, and 4-contrast 8-channel brain datasets using 1D random undersampling patterns (R = 4). MC-HTC and J-LORAKS applications for the T1W contrast dataset are equivalent to conventional single-contrast reconstruction, which produced obvious residual errors. Substantial reduction of aliasing artifacts can be observed in the joint reconstruction of T1W and T2W datasets and noise-like residuals were obviously suppressed for 3-, and 4-contrast jointly reconstructed compared to J-LORAKS. The error maps were displayed with enhanced brightness (×7) and corresponding NRMSE were shown.

Figure 4. Comparison to J-LORAKS reconstruction for T1W, T2W, FLAIR, and T1W-IR 8-channel datasets. The retrospective 1D random undersampling (R = 4) was performed independently for each contrast, which follows 1D Poisson-disc patterns.

The residual error maps were brightened (×7) for evaluating the performance of reconstruction and corresponding NRMSE were shown.

Figure 5. Histograms of residual error map corresponding to MC-HTC, J-LORAKS, and SAKE reconstruction using 1D random undersampling patterns (R = 4). MC-HTC joint reconstruction substantially reduced residual aliasing and noise amplification.

Figure 6. Joint reconstruction for T1W, T2W, FLAIR, and T1W-IR 8-channel datasets with 2D random undersampling patterns (R = 8). In this scheme, undersampling artifacts mainly appeared as noise-like residuals and were more effectively eliminated through MC-HTC.

Figure 7. Joint reconstruction for T1W, T2W, FLAIR, and T1W-IR 8-channel datasets using uniform undersampling patterns (R = 4) with the phase-encoding direction orthogonally alternated among contrasts. J-LORAKS reconstruction failed to remove extremely coherent aliasing, whereas MC-HTC still produced high-quality images.

Figure 8. NRMSE (averaged across 5 consecutive slices) for the reconstruction of 8-channel data undersampled with different undersampling patterns and acceleration factors ranging from 3 to 9. For both 1D/2D random undersampling, the lines represented reconstruction through MC-HTC (solid), J-LORAKS (dashed), and SAKE (dotted), respectively. For uniform undersampling, only MC-HTC was displayed (dash-dotted).

Figure 9. Evaluations of MC-HTC, J-LORAKS, and SAKE reconstruction of multi-contrast datasets with simulated rigid inter-scan motion. Only reconstructed T1W images were shown. (**A**) Reconstruction with 2-pixel displacement (corresponding to 2.4mm). (**B**) Reconstruction with 4-pixel displacement (corresponding to 4.8mm).

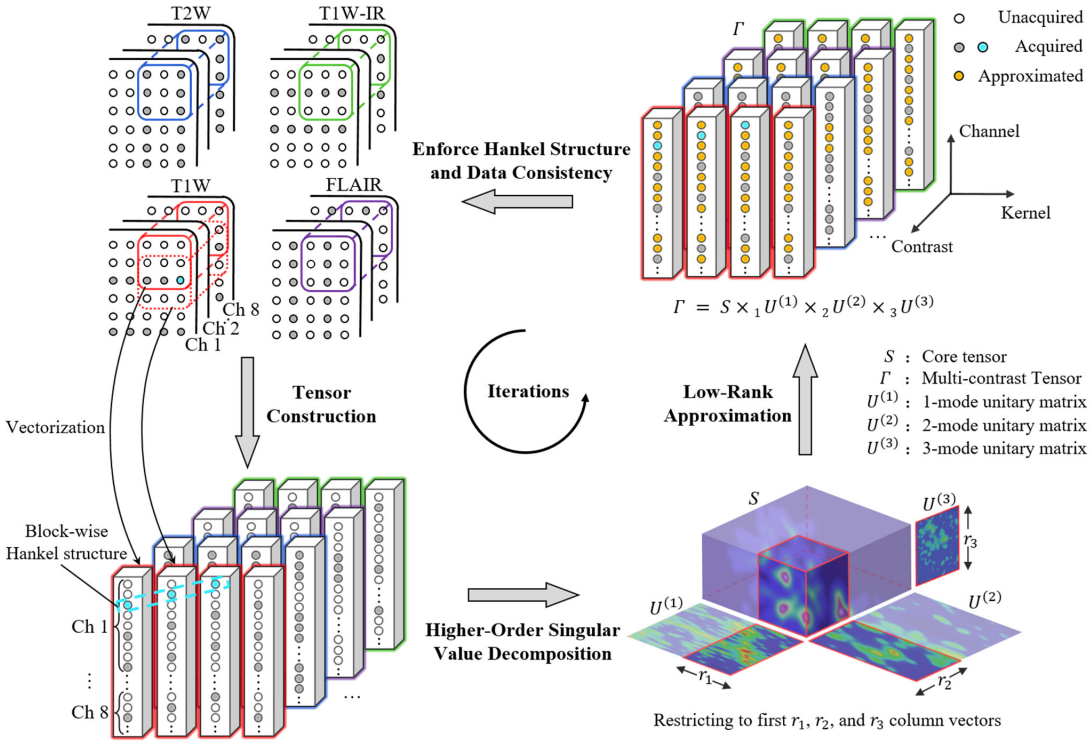

Figure 1

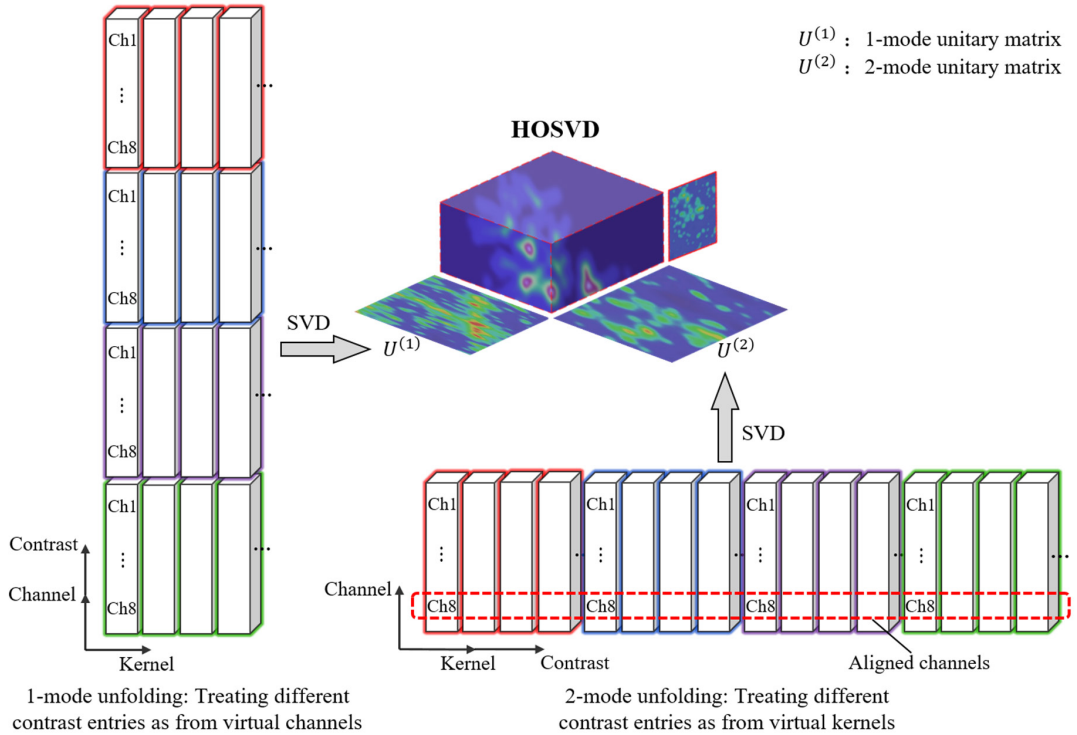

Figure 2

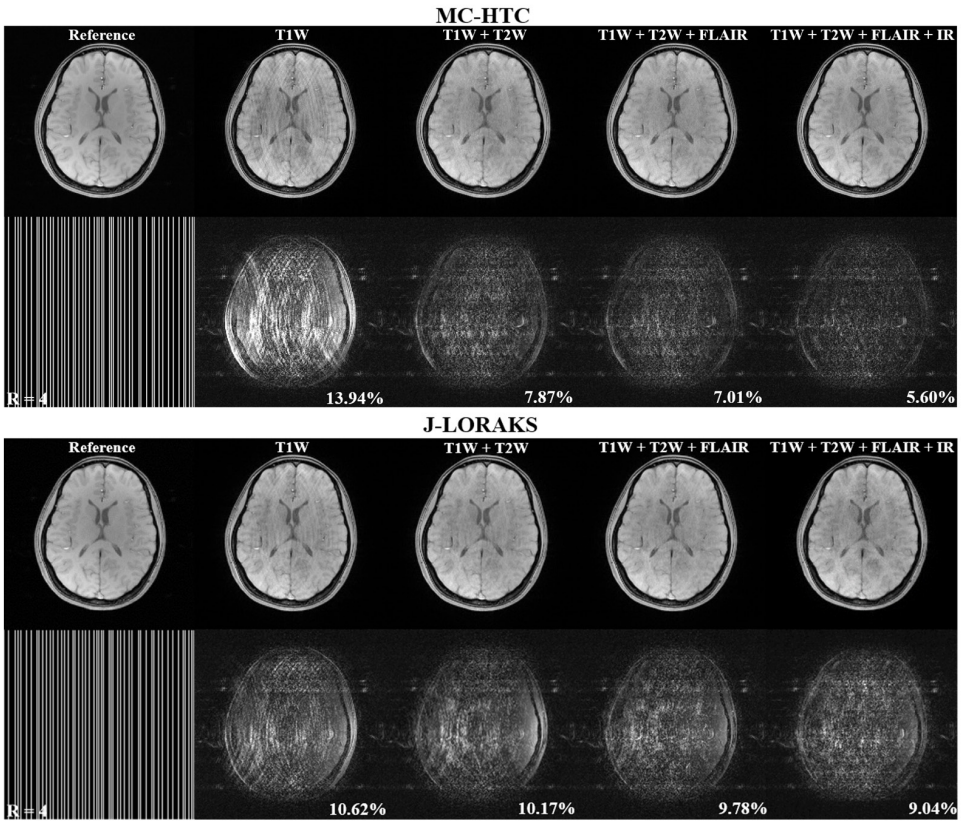

Figure 3

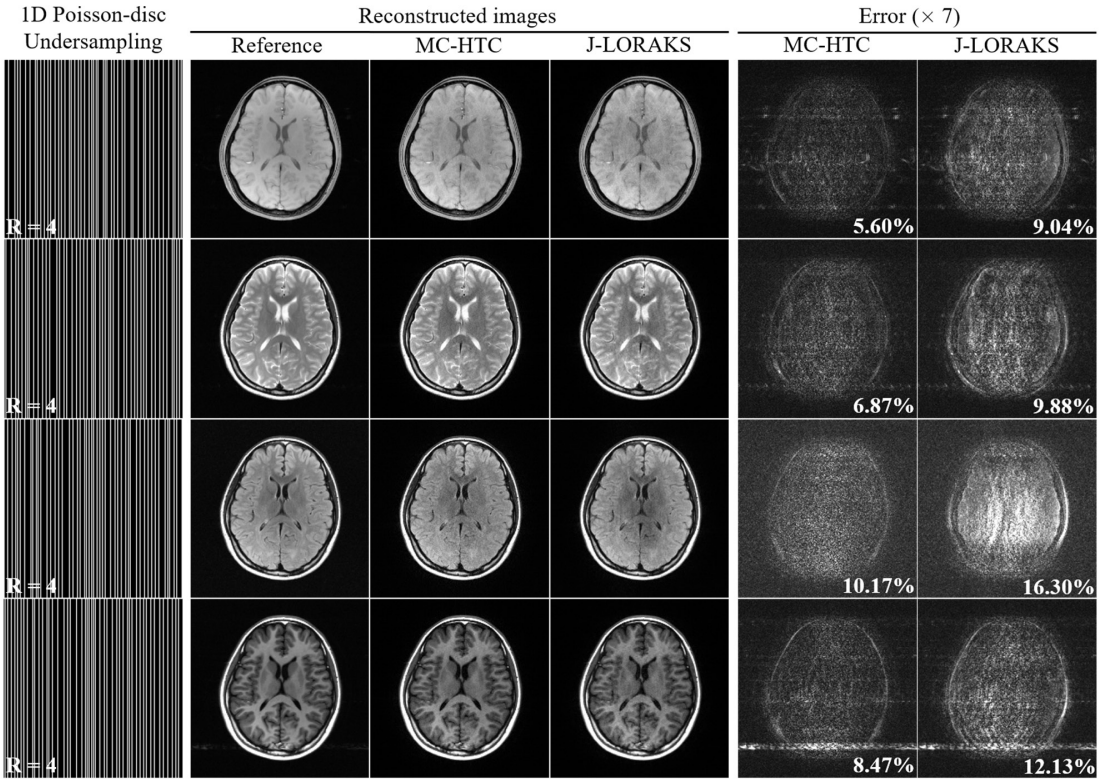

Figure 4

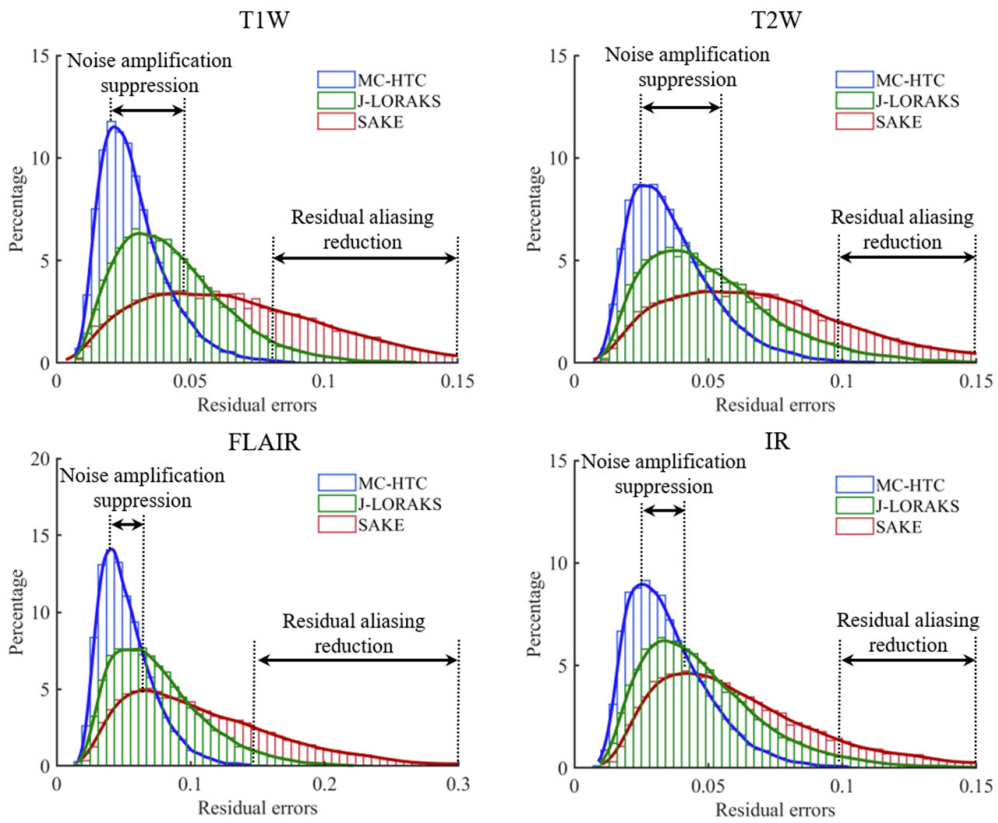

Figure 5

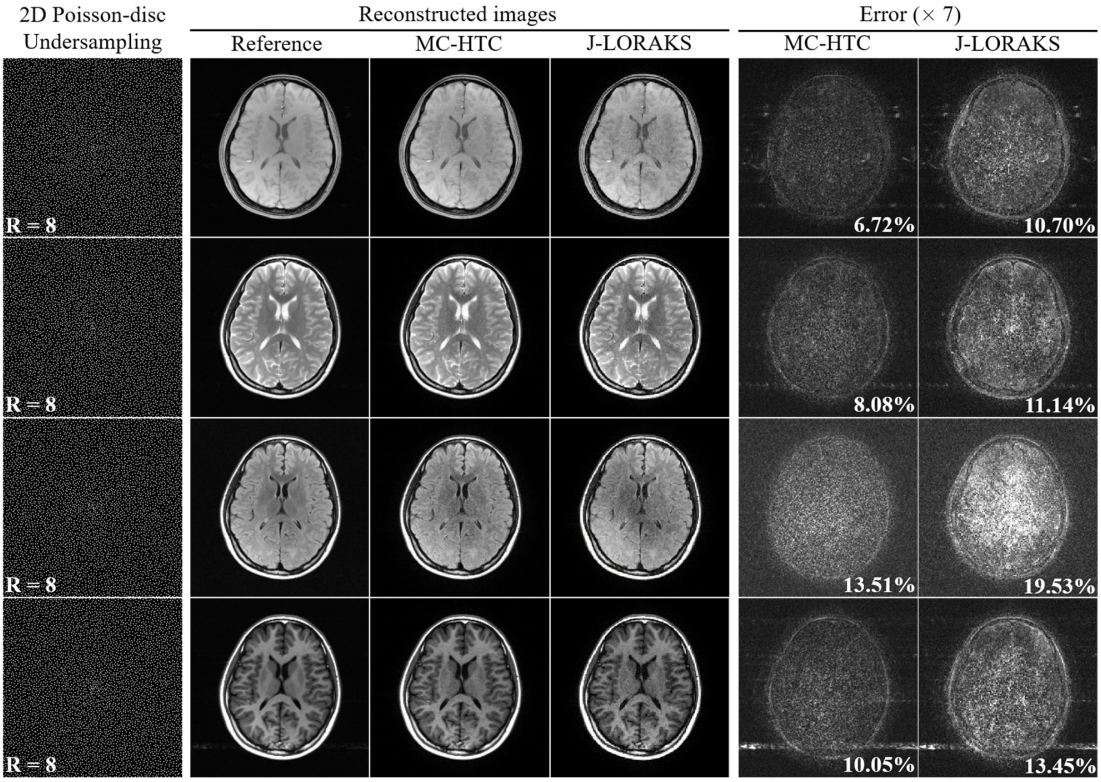

Figure 6

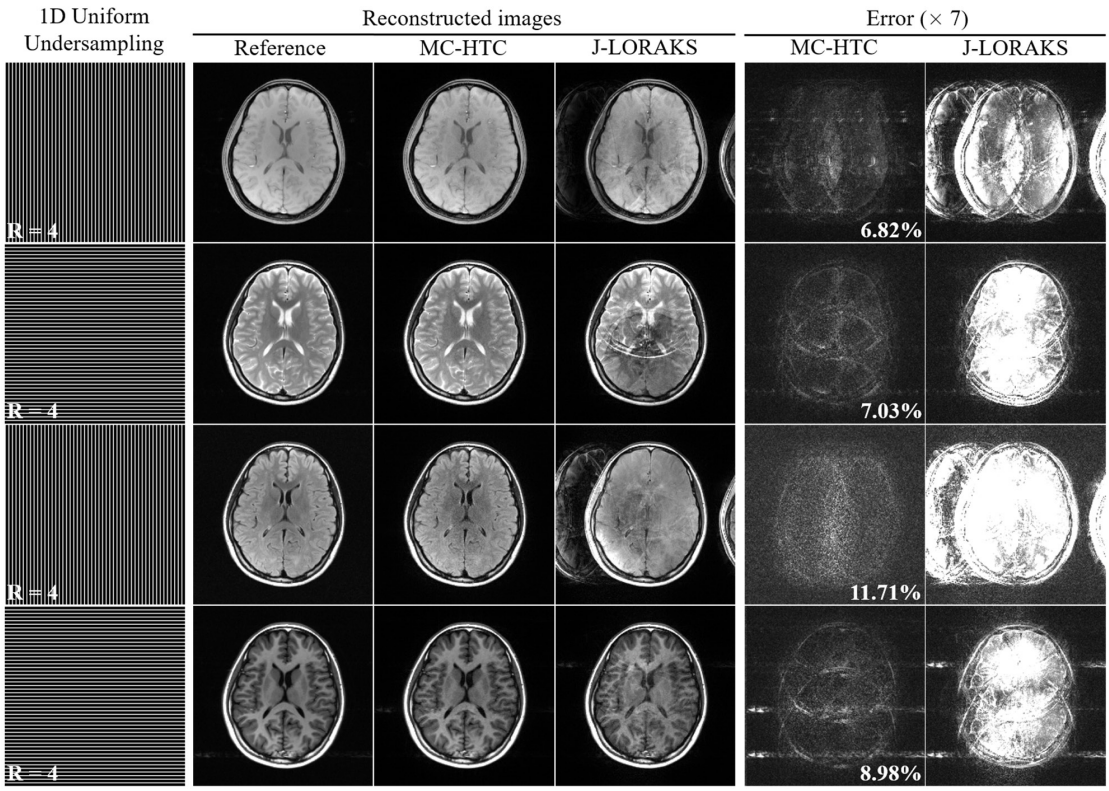

Figure 7

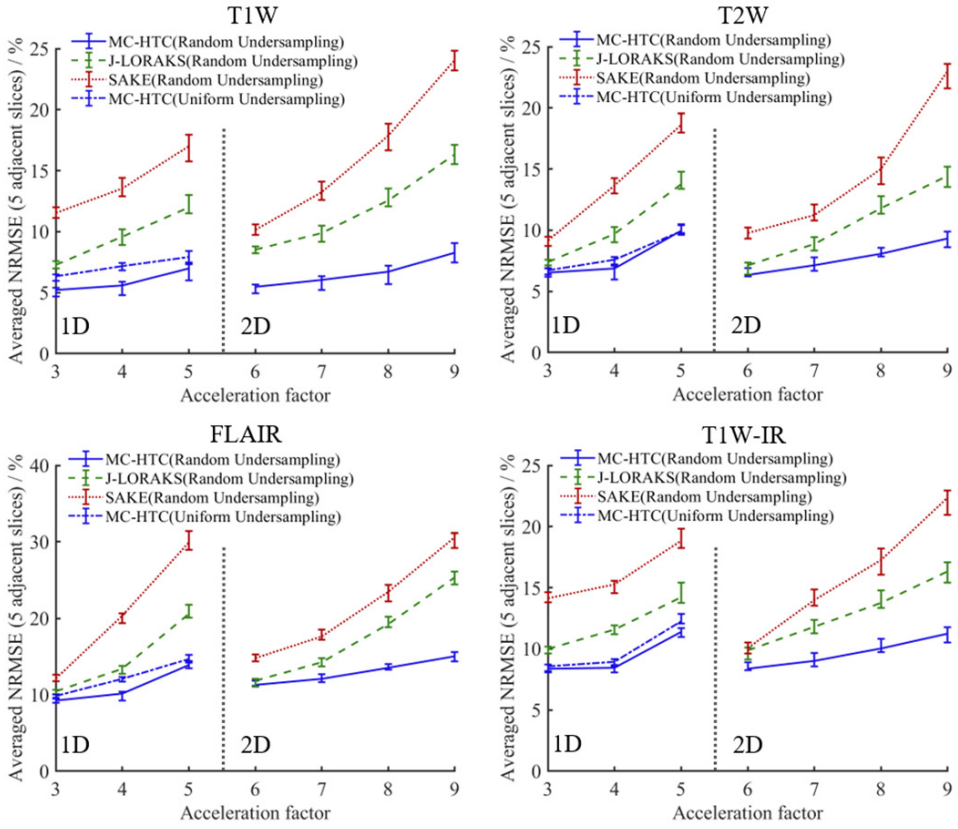

Figure 8

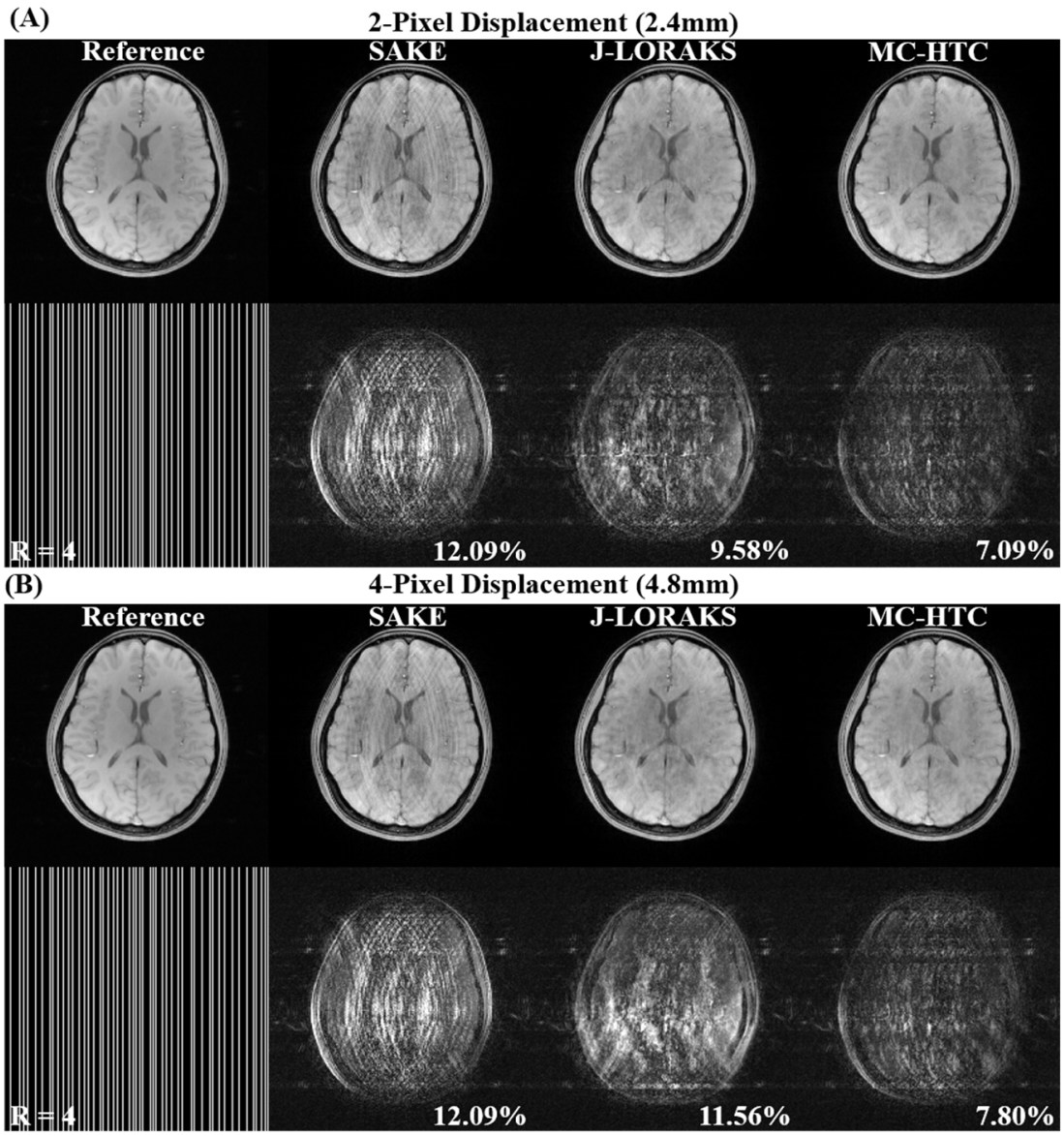
(A)
2-Pixel Displacement (2.4mm)
Reference
SAKE
J-LORAKS
MC-HTC
R = 4
12.09%
9.58%
7.09%
(B)
4-Pixel Displacement (4.8mm)
Reference
SAKE
J-LORAKS
MC-HTC
R = 4
12.09%
11.56%
7.80%

Figure 9